

Supporting Information
Balancing Sensitivity and Environmental Safety in
Fluorescent Probe Design: Improved Ethanol-thermal
Carbon Dots Enable a Leap in Mercury (II) Detection and
Zebrafish-Assessed Safety

submitted to

Analytical Methods

Xixuan Chen ^{a,b}, Lei Zheng ^{b*}, Rongzhen Ma ^c, Phong H.N. Vo ^d, Jiaxin Ni ^b, Songjun
Guo ^{a*}

a School of Resources, Environment and Materials, Guangxi University, Nanning
530004, PR China

b Chongqing Institute of Green and Intelligent Technology, Chinese Academy of
Sciences, Chongqing 400714, PR China

c School of Environment Science and Engineering, Sun Yat-Sen University,
Guangzhou 510080, PR China

d School of Natural Resource, Macquarie University, Sydney, NSW 2109, Australia

* Corresponding authors:

Email address: zhenglei@cigit.ac.cn (L. Zheng), guosj@gxu.edu.cn (S.J. Guo)

Text S1. Quantum Yield Measurements

The relative quantum yield (QY) of MUCDs was determined using quinine sulfate (QY = 54.6%¹ in 0.1 mol L⁻¹ H₂SO₄, $\lambda_{\text{ex}} = 350$ nm) as the reference. MUCDs in ethanol and the reference solution were diluted to absorbance < 0.05 at 350 nm to minimize inner filter effects². Fluorescence spectra were recorded at $\lambda_{\text{ex}} = 350$ nm with 5 nm excitation/emission slits. QY was calculated as:

$$\text{QY} = \text{QY}_{\text{ref}} \times \left(\frac{I_{\text{sample}}}{I_{\text{ref}}} \right) \times \left(\frac{A_{\text{ref}}}{A_{\text{sample}}} \right) \times \left(\frac{\eta_{\text{sample}}^2}{\eta_{\text{ref}}^2} \right) \quad (1)$$

where I is integrated fluorescence intensity, A is absorbance at 350 nm, and η is the solvent refractive index ($\eta_{\text{ref}} = 1.33$ for 0.1 mol L⁻¹ H₂SO₄).

Measurements were performed in triplicate at room temperature with the solvent background subtracted. To simplify the cumbersome traditional two-point calculation process, we developed an open-source platform based on Python3 called QY_Calculator, which enables rapid and automated determination of quantum yield.

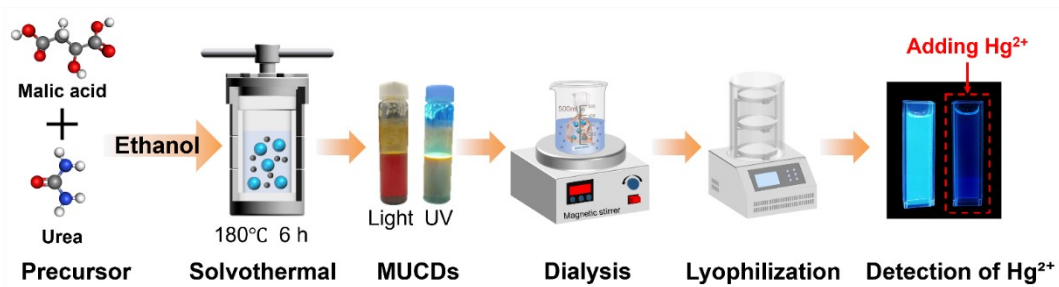


Fig. S1. Schematic flowchart for MUCDs synthesis and purification.

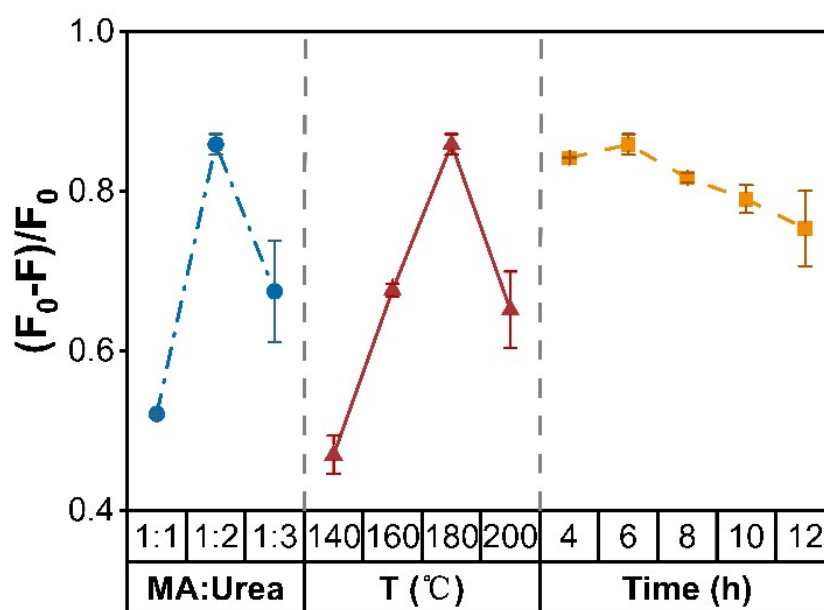


Fig. S2. Optimization of MUCDs synthesis conditions (malic acid: urea=1:2, 180 °C, 6 h).

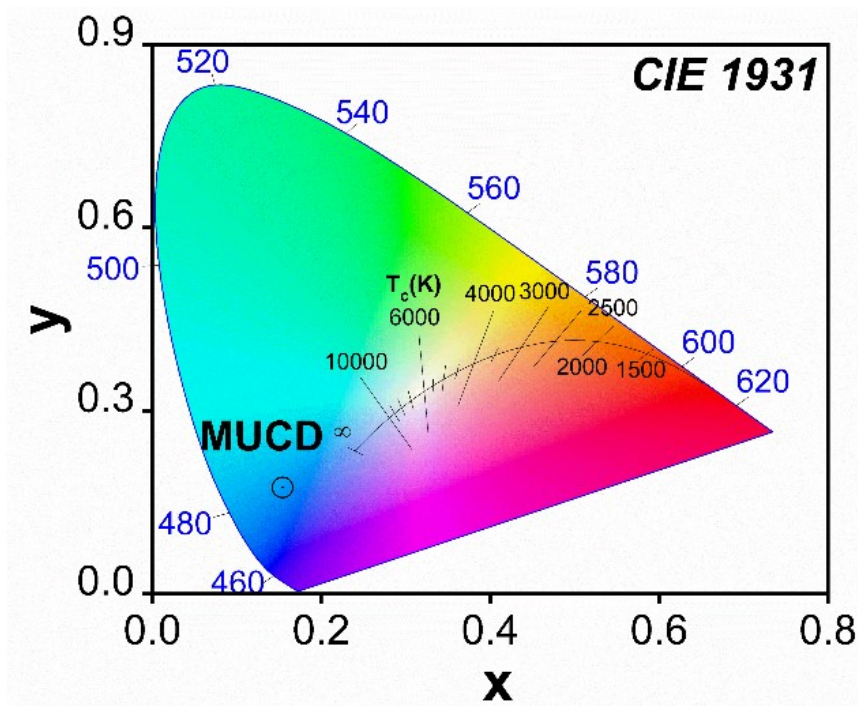


Fig. S3. CIE 1931 chromaticity diagram of MUCDs.

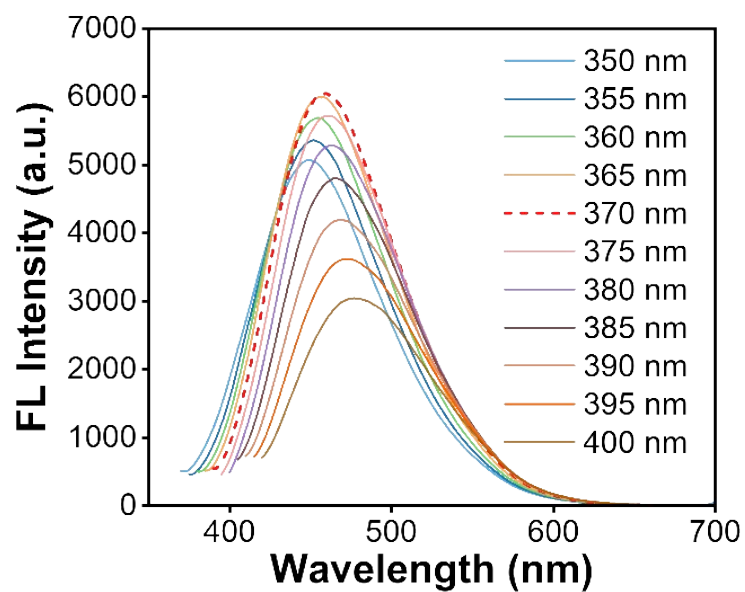


Fig. S4. Fluorescence spectra of MUCDs at different excitation wavelength (350-400 nm).

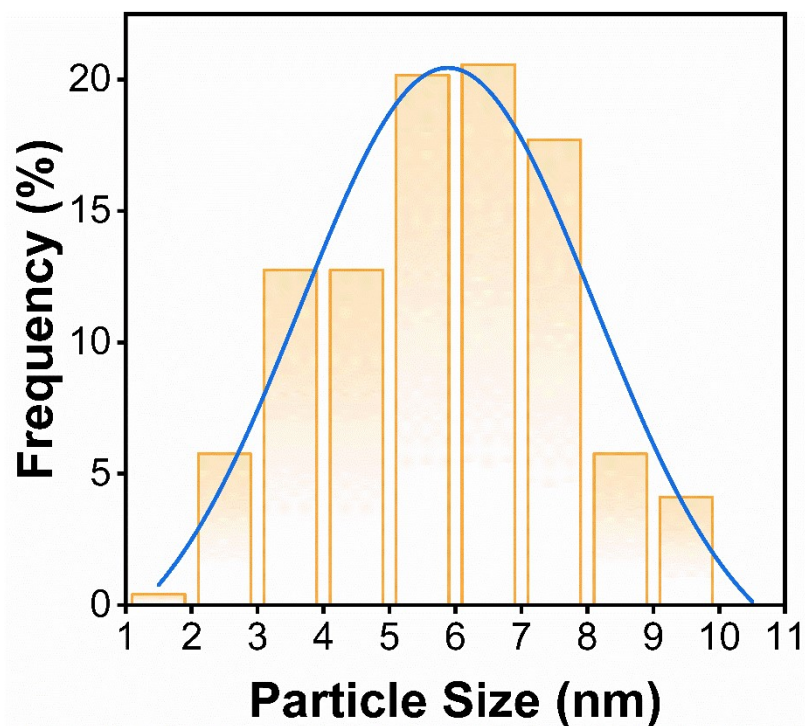


Fig. S5. Particle size distribution histogram (5-8 nm).

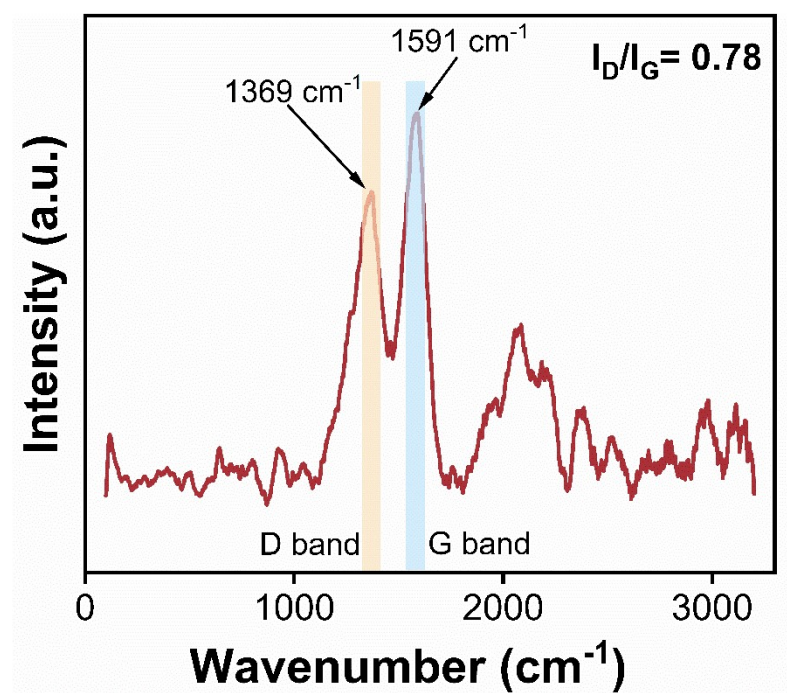


Fig. S6. Raman spectrum of the MUCDs.

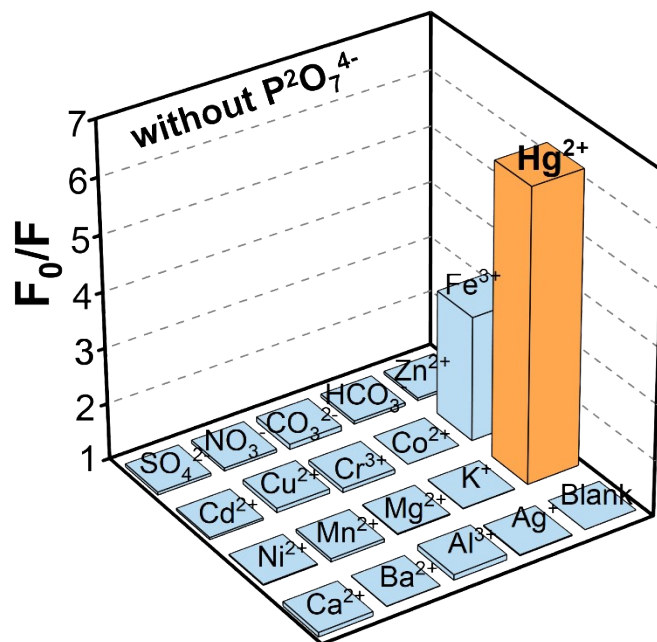


Fig. S7. Selectivity over interfering metal ions and anions ($50 \mu\text{mol L}^{-1}$ each) without $\text{P}^{2}\text{O}_7^{4-}$.

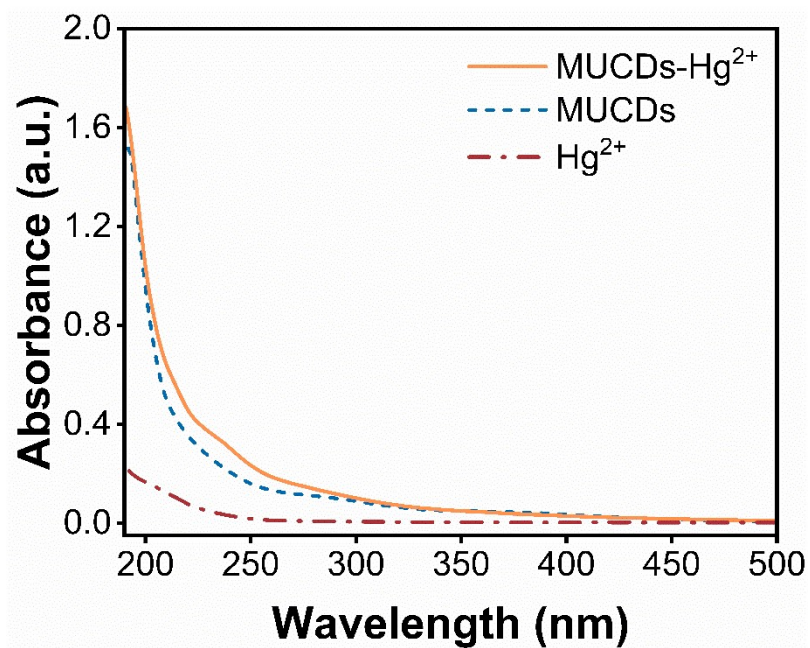


Fig. S8. The UV-Vis absorption spectra of MUCDs, MUCDs- Hg^{2+} and Hg^{2+} .

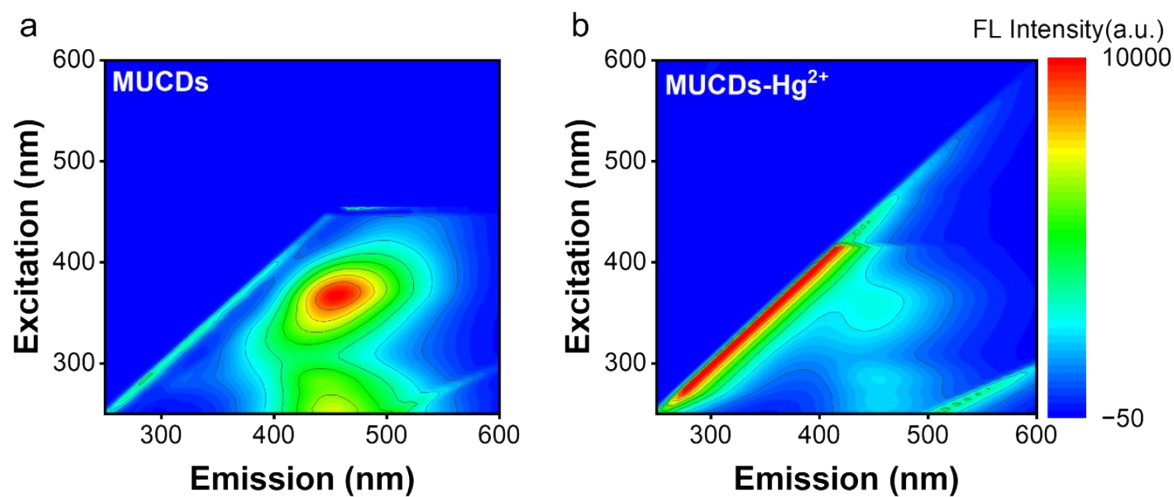


Fig. S9. 3D fluorescence spectra of MUCDs (a) and MUCDs-Hg²⁺ (b) excited at the wavelength.

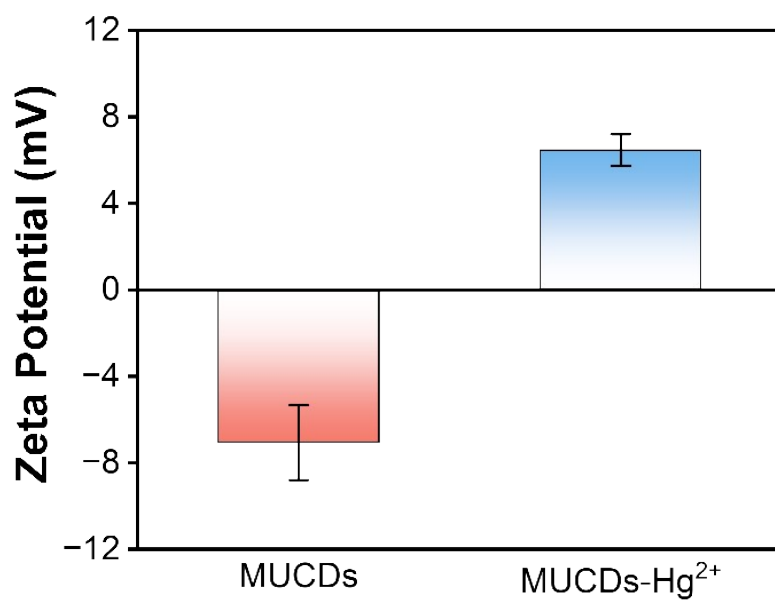


Fig. S10. Zeta potential analysis of MUCDs and the MUCDs-Hg²⁺ (n=3).

Table S1. Elemental composition and relative ratios of chemical bonds of MUCDs derived from XPS analysis.

Element	Atomic Content (%)	Chemical Bond	Bond Ratio (%)
C 1s	46.67	C-C / C=C	55.42
		C-N / C-O	21.03
		C=O	23.55
N 1s	16.24	N-C	89.70
		N-H	10.30
O 1s	37.08	C=O	70.89
		C-O	29.11

Table S2. Two-way ANOVA plot of MUCDs concentration and exposure time.

	Df	Sum Sq	Mean Sq	F value	P value
Concentration	6	0.73768	0.12295	243	<0.0001
Time	3	0.42429	0.14143	279.52941	<0.0001
Interaction	18	1.6778	0.09321	184.22876	<0.0001

At the 0.05 level, the overall mean of Concentration is significantly different.

At the 0.05 level, the overall mean of Time is significantly different.

At the 0.05 level, the interaction between Concentration and Time is significant.

References

- 1 J. W. Eastman, *Photochem. Photobiol.*, 1967, **6**, 55–72.
- 2 K. Nawara and J. Waluk, *Anal. Chem.*, 2017, **89**, 8650–8655.